SUPERCONDUCTING ACCELERATORS *

P. B. Wilson and H. A. Schwettman

High Energy Physics Laboratory
and
Department of Physics
Stanford University
Stanford, California

Summary

In this paper the application of superconductivity to several devices which conventionally require large amounts of rf power is considered. Design characteristics are given for superconducting electron linacs, cavities for electron synchrotrons, rf separators and microtrons.

Introduction

The usefulness of conventional electron and proton linear accelerators in nuclear and particle physics research is severely limited by low duty cycle. During the past several years the possibility of increasing the duty cycle of linacs by making the rf structure superconducting has been actively investigated. Banford and Stafford[1] have considered the feasibility of a superconducting proton linac. Measurements by Banford[2,3] and others[4,5] on superconducting surfaces have been performed in the frequency range of interest for proton linacs (200-600mc). At Stanford the possibility of superconducting electron linacs has been investigated; measurements on superconducting cavities near 3000 mc and the application of these results to the design of electron linacs have been published[6,7,8,9,10]. The related possibility of superconducting rf separators, which can match the inherent high duty cycle of a synchrotron, has also been proposed[11].

We will consider here the application of superconductivity to four devices which conventionally require large amounts of rf power: electron linacs, rf cavities for electron synchrotrons, rf separators, and microtrons. A more extensive treatment of the general problem of rf losses in superconducting surfaces, with application to the optimum choice of temperature, frequency and superconducting material can be found in Ref. 10.

Superconducting Electron Linacs

Operating Temperature

The existence of adequate refrigeration near the boiling point of liquid helium makes it attractive to operate a superconducting accelerator at 4.2°K. However, rf cavity measurements on superconducting lead surfaces indicate that operation at lower temperatures is highly desirable.

We have measured the Q of a electroplated lead cavity, operating at 2856 mc in the TE_{011} mode. In Fig. 1 the theoretical and measured dependence of the Q on temperature is shown. The theoretical temperature dependence has been obtained from a calculation[12], based on the BCS theory of superconductivity, which suggests that for the frequencies and temperatures of interest the surface resistance of a superconductor can be written as

$$R_s \propto \frac{1}{Q} \propto \frac{\omega^2}{T} e^{-\epsilon/kT} \qquad (1)$$

where 2ϵ is the gap in the energy spectrum of the superconductor. In Fig. 1, the deviation at low temperatures between the theoretical and measured Q's can be attributed to the presence of a residual resistance.

The rf power dissipated in a superconducting accelerator will be inversely proportional to the Q. From the measured temperature dependence the dissipation will decrease by a factor of 18 if the operating temperature is reduced from 4.2°K to 2°K. Operation at temperatures below 2°K cannot be justified unless further improvements are made in reducing the residual resistance of the electroplated surfaces. However, from Fig. 1 it is clear that the potential improvement increases rapidly at lower temperatures; an order of magnitude increase in Q is theoretically possible at 1.5°K.

Operation at 2°K or lower results in other benefits in addition to decreased losses. Below the lambda point (2.17°K) the helium bath is a superfluid with a thermal conductivity many times greater than room temperature copper. Heat from an accelerating structure can be transferred throughout the bath without introducing appreciable temperature gradients.

It should be noted that the measurements shown in Fig. 1 were obtained with a cavity which was magnetically shielded from external fields to a level of a few milligauss. At field levels comparable to the earth's field, the Q is significantly depressed. A superconducting accelerator operating at this temperature must therefore be magnetically shielded. Such shielding is easily accomplished and should pose no practical problem.

Refrigeration

The efficiency of the refrigeration process is an important consideration for high power superconducting devices. The total input power P_R into a refrigerator can be expressed as

$$P_R = \frac{300}{T\eta_p} P_S \qquad (2)$$

where P_S is the power dissipated in the accelerator structure. The factor T/300 represents the Carnot efficiency set by the second law of thermodynamics, while η_p represents how close the Carnot efficiency is approached in practice. At present large-scale refrigeration is not available at 2°K and values for η_p at this temperature can only be estimated. At 4.2°K existing large refrigerators operate at values of η_p of approximately 10%.

The cost of existing 4.2°K refrigerators can be represented by the relation

$$\text{Cost} \approx \$6{,}000\ P_S^{0.6} \qquad (3)$$

over the range 10 watts to 1 kilowatt. The cost of providing the same refrigeration at 2°K is expected to be about 3 times that given by the above relation.

Operating Frequency

According to Eq. (1), valid for frequencies below several kilomegacycles, the Q of a superconducting cavity varies as ω^{-2} at a given temperature. However, the shunt impedance per unit length r for an accelerating structure is the product of the unloaded Q times the geometry-dependent factor r/Q_o, which relates the axial electric field strength E to the energy stored per unit length w. By definition $r = E^2/(dP/dz)$ and $Q_o = \omega w/(dP/dz)$ and therefore,

$$\frac{r}{Q_o} = \frac{E^2}{\omega w}.$$

Since $w \propto E^2\lambda^2$, it is seen that r/Q_o varies as ω^1. The shunt impedance for a superconducting structure will therefore vary as ω^{-1}, and lower frequencies are desirable. This is in contrast to the case for room-temperature copper, where Q_o varies as $\omega^{-1/2}$, r varies as $\omega^{1/2}$, and higher frequencies are favored.

As the frequency is decreased the diameter of the structure becomes inconveniently large. Furthermore, the rf structure of the beam may become evident for some experiments. For such reasons a few hundred megacycles will probably be a lower limit to acceptable frequencies.

Energy Gain

The shunt impedance per unit length of a slow-wave structure is defined as

$$r = \frac{E^2}{dP/dz} \qquad (4)$$

where dP/dz is the power dissipated per unit length for a traveling wave, and E is taken to be the fundamental space harmonic component of the wave. For a superconducting traveling-wave (TW) structure the attenuation of the wave is negligible and the energy gain for a particle riding the crest of the wave is obtained by integrating the above expression.

$$V_{TW} = \sqrt{rLP_S} \qquad (5)$$

For a standing wave (SW) device, twice the power is needed to produce a given energy gain, and

$$V_{SW} = \sqrt{\frac{1}{2}\, rLP_S}\ . \qquad (6)$$

The advantages of TW operation are readily apparent. The SW structure requires twice the power to produce a given energy gain. Stated another way, the peak field is approximately twice the average field seen by the particle. If the energy gradient is limited by a critical field, then the maximum gradient in the TW case will be twice that allowed in the SW case. However, a superconducting TW structure in practice must be a resonant ring. Such a device is considerably more complex to construct than a resonant cavity.

Beam Loading

Relations can be written for the energy gain in the general case where beam loading, phasing, cavity tuning, and cavity coupling are taken into account. Consider first the cavity voltage produced by the rf generator with the beam off. This can be written for the SW case as

$$V_g = \sqrt{\frac{1}{2}\, rLP_o}\ \frac{2\sqrt{\beta}}{1+\beta}\cos\psi\ . \qquad (7)$$

Here P_o is the incident power, β is the coupling coefficient ($\beta = 1$ at match) and ψ is a tuning parameter given by

$$\psi = -\tan^{-1}(2\, Q_L \delta) \qquad (8)$$

where $\delta = (\omega - \omega_o)/\omega_o$.

Equations (7) and (8) can be derived from the parallel resonant circuit representation for the cavity which is shown in Fig. 2. The derivation assumes that the incident power P_o corresponds to the available power from the source generator I_g, and that the cavity shunt conductance G_c is $4/rL$. For $\psi = 0$ and $\beta = 1$, Eq. (7) then reduces, as it should, to Eq. (6).

If now the rf generator is turned off and a relativistic bunched beam is sent through the cavity, a voltage will be induced which is

$$V_b = \frac{i_o rL}{4}\ \frac{2}{1+\beta}\cos\psi\ . \qquad (9)$$

Tight bunches have been assumed so that the amplitude of rf beam current is twice the dc component i_o .

The net cavity voltage produced when both the generator and the beam are on can now be obtained by a vector addition of the voltages given in Eqs. (7) and (9). The component of this voltage in phase with the beam current gives the energy gain of the electron bunches. From Fig. 3 this is

$$V = V_g \cos(\theta + \psi) - V_b \cos \psi \qquad (10)$$

where the angle θ is the phase of the source generator measured with respect to the bunched beam. Clearly the tuning and phasing are interrelated. For example, if the cavity is detuned, it is possible to compensate partially by adjusting the phase so that $\theta = -\psi$.

From this point on we will discuss only the on-resonance, in-phase case. Equations (7), (9) and (10) now can be combined to give the energy gain,

$$V = \sqrt{\frac{1}{2} rLP_o}\ \frac{2\sqrt{\beta}}{1+\beta} - \frac{i_o rL}{2(1+\beta)} \ . \qquad (11)$$

It is seen that the beam energy decreases linearly with beam current until it reaches zero when the two terms in Eq. (11) are equal. The efficiency, defined by $\eta = i_o V/P_o$, increases as current is increased until it reaches a maximum when the beam energy is one-half its unloaded value. The behavior of both energy and efficiency as a function of current is similar to that for a conventional electron linac. At the optimum efficiency with respect to current we have

$$V_{opt} = \sqrt{\frac{1}{2} rLP_o}\ \frac{\sqrt{\beta}}{1+\beta}$$

$$i_{opt} = \sqrt{\frac{2 P_o \beta}{rL}}$$

$$\eta_{opt} = \frac{\beta}{1+\beta}$$

The efficiency is seen to approach unity for large values of β .

The power dissipated in the structure at optimum efficiency can be obtained by equating V_{opt} to Eq. (6).

$$\frac{P_S}{P_o} = \frac{\beta}{(1+\beta)^2} \rightarrow \frac{1}{\beta} \, . \qquad (12)$$

The power reflected from the cavity at optimum efficiency is now readily calculated from conservation of power as $P_R/P_o = (1+\beta)^{-2}$. It will be very small for large β .

Loaded Q and Filling Time

For reasonable energy gradients, the power dissipated in the structure of a superconducting accelerator will be small. Under normal operating conditions most of the input power will go into the beam. For this case $P_B \approx P_o$, $\beta \gg 1$, and Eq. (12) leads to

$$Q_L \approx \frac{Q_o}{\beta} \approx \frac{Q_o P_S}{i_o V} \, .$$

By combining this with Eq. (6) we obtain

$$Q_L \approx \frac{2\,(V/L)}{i_o (r/Q_o)} \ . \qquad (13)$$

the loaded Q is important because it determines the filling time T_F , given by $T_F = Q_L/\omega$.

Limits on the Energy Gradient

As in a conventional linac, electric breakdown will impose a practical limit on the energy gradient. In a superconducting accelerator additional limits on the gradient must be considered. One of these is set by the critical magnetic field for a superconductor. For dc magnetic fields, the superconductor reverts to the normal state at a field given by

$$H = H_o\,(1 - t^2)$$

where $t = T/T_c$ and T_c is the critical temperature. In a typical SW disk-loaded structure the maximum magnetic field at the wall of the structure is related to the voltage gain per unit length by

$$H(\text{gauss}) \approx .004\ \frac{V}{L}\ (\text{volts / cm}) \qquad (14)$$

For the TW case the maximum magnetic field is only one-half that given by Eq. (14) for a given energy gradient. For superconducting lead and niobium the critical magnetic field does not impose a severe limitation on the gradient. Taking the dc critical field for lead (H_o= 800 gauss) and niobium (H_o = 1960 gauss), the maximum energy gradient for an accelerator operating at 2°K is given in the following table:

	SW	TW
Pb	5.5 MeV/ft	11 MeV/ft
Nb	14	28

Measurements on electroplated lead surfaces have been extended up to one-half of the dc critical field without enhanced losses. Preliminary measurements on superconducting tin indicate that rf magnetic fields in excess of the dc critical field may be supported.

The numbers in the preceeding Table can be contrasted with the maximum energy per unit length of circumference in a synchrotron. For a magnetic field of 14 kilogauss, this is 20 MeV/ft. The effective energy per unit length is always less, since in practice not all of the circumference can be occupied by field. For example, it is 13 MeV/ft for the Brookhaven AGS at maximum energy.

Another limit on the energy gradient in a superconducting accelerator exists. When high power is put into an accelerator structure, the thermal impedance of the copper in the structure and the Kapitza resistance for the transfer of heat across the interface between the copper and the helium bath will result in a temperature rise of the superconducting surface. Associated with the temperature rise will be a shift in the resonant frequency of the cavity. This comes about because of the variation with temperature of the superconducting penetration depth λ_p. Since λ_p varies as

$$\lambda_p(t) = \lambda_p(0)[1 - t^4]^{-1/2}$$

the frequency is much less sensitive to temperature variations at low temperatures. For temperatures well below T_c, $d\lambda_p/dt$ is proportional to t^3. For stable operation there will be a maximum allowable temperature rise and hence a maximum allowable value of P_S/L. An approximate calculation indicates that this effect places a limit on the energy gradient of 10 to 15 MeV/ft.

Examples

The preceeding discussion can be applied to the design of typical superconducting linacs. Machine A in Table I is a short, low-energy accelerator suitable for nuclear physics. Machine B is an accelerator of intermediate energy and might be a superconducting version of the Stanford Mark III. Machine C could represent a superconducting version of the two-mile-long SLAC accelerator. Traveling-wave operation has been assumed at a frequency of 1 kmc. The unloaded Q for the structure is based on the measured value at 2856 mc, and is estimated to be 7×10^9 at 1 kmc and 2°K. For a disk-loaded structure $r/Q_o \approx 450/\lambda$, which at 1 kmc is 15 ohms/cm. The refrigeration and rf power specified in these examples have been chosen as being economically reasonable.

In pulsed operation, the long filling times necessitate klystron pulses of the order of one second. For pulses of such length, klystrons cannot be operated at power levels higher than their cw rating. This means that, for a constant refrigeration power, the average beam current will vary as $(V_{pulsed}/V_{cw})^{-3}$. This effect is evident in the examples.

Superconducting Cavities for Synchrotrons

The use of superconducting cavities can increase the maximum energy of an electron synchrotron if, using conventional cavities, the synchrotron is rf-limited rather than magnet-limited. For a given circulating current, the power lost to synchrotron radiation varies as E^4/ρ, where E is the energy and ρ the radius. The power dissipated in the cavities, however, increases as E^8 and at some energy will become the dominate loss. The maximum synchrotron energy will then be set by practical limits on the size of the rf system.

The proposed 10 GeV Cornell synchrotron is an example of a machine limited by the rf system. In Table II the design of a conventional rf system is given[13] for operation at the 10 GeV level. It is seen that the power dissipated in the cavities is a factor of 6 greater than the power going into synchrotron radiation. Also given in the Table is the design of a superconducting rf system capable of increasing the energy of this machine to 15 GeV, which is still within the capability of the magnets. The refrigeration requirement even at 4.2°K is modest.

The filling time for the superconducting cavities is based on optimum power transfer to the beam at maximum energy. The coupling coefficient for this condition, and hence the loaded Q and the filling time, can be calculated for the specified phase with the aid of the vector diagram in Fig. 3 ($\psi = 0$, $\varphi = 30°$). The filling time is seen to be acceptably short compared to the accelerating time of approximately 8,000 μ sec.

Superconducting rf Separators

Rf separators usually provide the best means for obtaining physical separation of particles at momenta greater than about 10 GeV/c. In order to produce the intense fields required for the separation of particles with high momenta, a conventional rf separator must be fed with tens of megawatts of rf power and therefore must be operated on a pulsed basis. However, a separator pulsed for only a few microseconds does not provide a good match to a synchrotron for many experiments. Use of a superconducting separator structure immediately comes to mind.

An rf separator structure is in many ways similar to a traveling-wave linac structure, except that there is a transverse magnetic deflection field on the beam axis instead of a longitudinal electric accelerating field. A transverse shunt impedance $r_\perp$ can be defined for a separator structure in analogy with Eq. (4):

$$r_\perp = \frac{E_\perp^2}{dP/dz} .$$

Here $E_\perp$ is an equivalent deflecting electric field strength. By integrating the above relation for a low-loss standing-wave structure, we arrive at the total transverse momentum in eV/c imparted to the beam,

$$V_\perp = \sqrt{\frac{1}{2} r_\perp L P_S} \quad . \qquad \text{(SW)} \qquad (15)$$

Again, P_S represents the total power dissipated in the structure, and the factor of 1/2 is missing for the TW case.

As in the case of the superconducting linac, there are conflicting requirements on the operating frequency of a superconducting separator. The refrigeration power will be reduced if the frequency is low and in addition the acceptance increases as λ^2 . There is one strong argument for higher frequencies. For some separation systems, the particles must be allowed to drift until a phase shift of 180° takes place between particles of slightly different velocities. Therefore, the necessary drift distance will increase in direct proportion to the operating wavelength. An S-band frequency provides a reasonable compromise between the drift distance and the acceptance. At 3 kmc the disk hole diameter is about one inch, and the drift distance needed to produce a half cycle phase shift between protons and π's at 20 GeV/c is 50 meters.

Measurements at SLAC[14] give $r_t = 1.1 \times 10^5$ Ω/cm as typical for a room-temperature copper separator structure operating in the TM_{11}-like (or HEM_{11}) mode. To produce a transverse momentum of 20 MeV/c in a structure 3 meters in length, we find using Eq. (15) that a power P_S of 400 watts is required. This assumes the measured Q improvement factor of 6×10^4 for lead at 2°K.

The preceeding values of frequency, transverse momentum, and drift length are those which have been chosen to achieve p-π separation at 20 GeV/c with the CERN separator now under construction[15] . This separator uses conventional cavities, which require 17 MW of peak rf power per cavity. In Table III the parameters of the superconducting separator are shown. If a 5% duty cycle is assumed, which matches that of the synchrotron, the refrigerator input power is about 80 kw for the two cavities required.

By assuming pulsed operation to reduce the refrigeration requirement another problem has been introduced. If the cavities are critically coupled, the unloaded Q is about 6×10^8 and the filling time is therefore 16 ms. For a synchrotron operating at one pulse per 5 seconds, a 5% duty cycle implies a spill-out time of 100 ms. The filling time is then an unacceptably large fraction of the spill-out time. By increasing β to 30, the filling time is reduced to 1 ms and the required peak klystron power is increased to 3 kw, which is still tolerable. The filling time for a critically-coupled superconducting cavity scales as λ^3 , so the problem becomes rapidly worse at lower frequencies.

Superconducting Microtrons

A microtron is constructed by mounting an accelerating cavity at the periphery of a uniform magnetic field. The electrons move on orbits of increasing radii, and if the cavity voltage and magnetic field are properly chosen, the electrons will return at the correct phase for maximum energy gain on each revolution. The relation between the operating wavelength and magnetic field can be shown to be[16]

$$B\lambda = \frac{10{,}700}{\mu-\nu} \text{ gauss-cm}$$

where μ and ν are integers. For a superconducting microtron the choice of $\mu - \nu = 1$ is reasonable. This condition gives the strongest magnetic field and, since $B\rho \propto E$ for relativistic particles, the smallest magnet radius for a given energy. This choice also implies that the energy gain on each passage through the cavity must be ν times the rest mass of the electron. Higher values of ν imply fewer turns and a wider separation between orbits. The separation is reasonable even for $\nu = 1$, and for this case the energy gain per turn becomes 0.51 MeV.

Taking the finite transit angle into account, the energy gain of a relativistic particle passing through a TM_{010}-mode cylindrical cavity of height h and axial field E_0 can be written

$$V = E_0 h \frac{\sin(\pi h/\lambda)}{\pi h/\lambda} .$$

As a function of h , the energy gain is maximum when $h = \lambda/2$. For this condition the power required for V = 0.51 MeV can be calculated for the TM_{010} mode to be

$$P_S = \frac{2.3 \times 10^5}{\lambda(\text{cm})\ Q/Q_{300}} . \qquad (16)$$

Since Q/Q_{300} varies as $\lambda^{3/2}$, the required power varies as λ^{-2} and lower frequencies are favored. However, the magnet diameter for a given energy is proportional to λ .

At 3 kmc and 2°K, $Q/Q_{300} = 6 \times 10^4$ and from Eq. (16) the power dissipation in the cavity is 1.2 watts. This is a very modest refrigeration requirement and it is reasonable to dispense with a refrigerator altogether, using a stored supply of liquid helium instead. Twenty liters would be adequate for a ten hour run.

In Table IV design parameters are given for two microtrons. It is seen that the 6 kmc microtron has a more compact magnet for a given energy. At this frequency a magnet diameter of 1 ft/10 MeV is required.

Acknowledgment

The authors wish to acknowledge the participation of Prof. W. M. Fairbank in all phases of the superconducting accelerator program at Stanford.

References

1. A. P. Banford and H. G. Stafford, J. Nucl. Energy, Part C 3, 287 (1961).
2. A. P. Banford, Proceedings of the International Conference on High Energy Accelerators, Dubna, 1963 (Atomizdat, Moscow, 1964) p. 541.
3. A. P. Banford, 1964 Cryogenic Engineering Conference, Philadelphia, Penn. To be published in Advances in Cryogenic Engineering, Vol. 10.
4. A. Susini, "Initial Experimental Results Concerning Superconductive Cavities at 300 Mc/s", CERN Internal Report 63-2, MCS Division (February 1963).
5. J. Rüfenacht and L. Rinderer, Z. Angew. Math. u. Physik 15, 192 (1964).
6. P. B. Wilson, Nucl. Instr. Methods 20, 336 (1963).
7. W. M. Fairbank, J. M. Pierce and P. B. Wilson, Proceedings of the Eighth International Conference on Low Temperature Physics, London, 1962 (Butterworths, Washington D.C., 1963) p. 324.
8. P. B. Wilson, H. A. Schwettman and W. M. Fairbank, Proceedings of the International Conference on High Energy Accelerators, Dubna, 1963 (Atomizdat, Moscow, 1964) p. 535.
9. J. M. Pierce, H. A. Schwettman, W. M. Fairbank, and P. B. Wilson, Proceedings of the Ninth International Conference on Low Temperature Physics, Columbus, Ohio, 1964 (to be published).
10. H. A. Schwettman, P. B. Wilson, J. M. Pierce and W. M. Fairbank, 1964 Cryogenic Engineering Conference, Philadelphia, Penn. To be published in Advances in Cryogenic Engineering, Vol 10.
11. B. W. Montague, "The Application of Superconductivity to R. F. Particle Separators", CERN Internal Report. AR/Int. PSep/63-1 (January 1963).
12. A. A. Abrikosov, L. P. Gor'kov and I. M. Khalatnikov, Zh. Eksperim. i Teor. Fiz. 35, 265 (1958) [English transl.: Soviet Phys. -- JETP 8, 182 (1959)].
13. M. Tigner, Private communication.
14. O. A. Altenmueller, R. R. Larsen and G. A. Loew, "Investigations of Traveling-wave Separators for the Stanford Two-Mile Linear Accelerator", SLAC Report 17, Stanford Linear Accelerator Center, Stanford, Calif. (August 1963).
15. M. Bell, P. Bramham, R. D. Fortune, E. Keil and B. W. Montague, Proceedings of the International Conference on High Energy Accelerators, Dubna, 1963 (Atomizdat, Moscow, 1964) p. 798.
16. J. J. Livingood, Principles of Cyclic Particle Accelerators, (D. Van Nostrand Company, Inc., New York, 1961) pp. 189-194.

Footnotes

* Work supported in part by Office of Naval Research, Contract Nonr 225 (67).

TABLE I

SUPERCONDUCTING LINAC DESIGNS

f = 1 kmc   T = 2.0°K   TW case

	A	B	C
Energy (cw)	80 MeV	1.0 GeV	20 GeV
Length	20 ft	300 ft	10,000 ft
Current (cw)	250 μa	300 μa	250 μa
Max pulsed energy (E_{max})	220 MeV	3.3 GeV	110 GeV
Duty cycle at E_{max}	12%	10%	3%
Ave. current at E_{max}	12 μa	9 μa	1.5 μa
Refrig. power at 2°K	100 watts	1.2 kw	13 kw
Input power to refrig.	200 kw	2.4 Mw	26 Mw
Est. refrig. cost	$350,000	$\$1.5 \times 10^6$	$\$10 \times 10^6$
Beam power (cw)	20 kw	300 kw	5 Mw
Input power to klystrons (cw)	50 kw	750 kw	12.5 Mw
No. 20 kw klystrons	1	15	250
β (cw)	200	250	385
Q_L (cw)	3×10^7	3×10^7	2×10^7
T_F (cw)	5 ms	5 ms	3 ms
β at E_{max}	25	25	13
Q_L at E_{max}	3×10^8	3×10^8	5×10^8
T_F at E_{max}	50 ms	50 ms	80 ms

TABLE II

CONVENTIONAL AND SUPERCONDUCTING RF SYSTEMS FOR AN ELECTRON SYNCHROTRON

	Conventional	Superconducting (4.2°K)
Maximum energy	10 GeV	15 GeV
Max. synch. rad. loss/turn	8.85 MeV	45 MeV
Max. power into sync. rad.	60 kw	315 kw
Max. cavity voltage (4 cavities)	10.8 MeV	55 MeV
Max. power dissipated in cavities	420 kw	325 watts
Input power to rf system (ave.)	360 kw	290 kw
Input power to refrigerator	--	100 kw
Cavity mode	$2\pi/3$ TW	$2\pi/3$ SW
Unloaded Q	31,000	1.5×10^9
Shunt impedance / unit length	2.2×10^7 Ω/meter	1.1×10^{12} Ω/meter
r/Q_o	7.2 Ω/cm	7.2 Ω/cm
Loaded Q	--	1.0×10^6
Filling time	1.5 μ sec	340 μ sec
Coupling coefficient	--	1500
Est. refrigerator cost	--	$150,000

General:

Synchrotron radius	100 meters
Rf frequency	476 mc
Cavity length	4×4.2 meters
Phase angle	120°
Circulating current	7 ma
Repetition rate	60 pps
Rf duty cycle	30%
Rf efficiency (est.)	40%

TABLE III

SUPERCONDUCTING RF SEPARATOR

Operating frequency	2856 mc
Peak transverse momentum per cavity	20 MeV/c
Length	3 m
Mode	$2\pi/3$ SW
Temperature	2.0°K
Duty cycle	5%
Q_o	6×10^8
Peak rf power per cavity	400 watts
Average power per cavity	20 watts
Refrigerator power (2 cavities)	80 kw
Approx. refrigerator cost	$150,000
Coupling coefficient β	30
Loaded Q	2×10^7
Filling time	1 ms
Peak klystron power per cavity	3 kw
Peak magnetic field at wall (est.)	330 gauss

TABLE IV

EXAMPLES OF SUPERCONDUCTING MICROTRONS

	A	B
Energy	50 MeV	100 MeV
Frequency	3000 mc	6000 mc
Magnet radius	1.57 meters	1.57 meters
Magnetic field	1070 gauss	2140 gauss
Resonance parameters	$\nu=1$, $\mu=2$	same
Orbit separation	3.2 cm	1.6 cm.
Energy gain/turn	0.51 MeV	0.51 MeV
Cavity transit angle	π radians	π radians
Peak cavity voltage	0.80 MeV	0.80 MeV
Operating temperature	2.0°K	2.0°K
Power dissipated in cavity	1.2 watts	5 watts
Klystron power	10 kw	10 kw
Beam current	200 μa	100 μa
Coupling coefficient	8,000	2,000
Unloaded Q	1.1×10^9	2.7×10^8
Loaded Q	1.3×10^5	1.3×10^5
Peak rf magnetic field	275 gauss	550 gauss

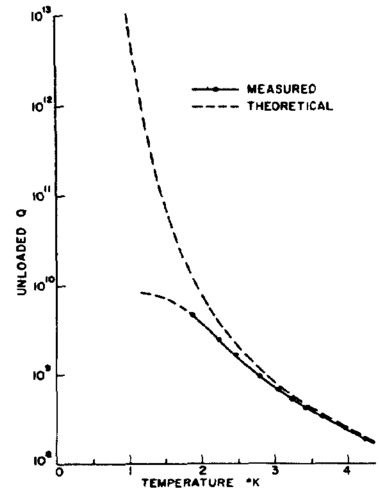

Fig. 1. Theoretical and measured cavity Q as a function of temperature.

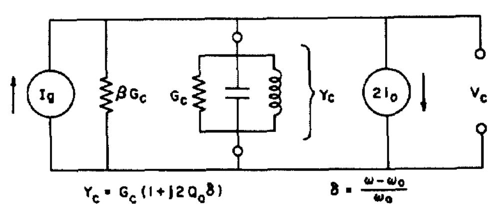

Fig. 2. Equivalent circuit for a beam-loaded cavity.

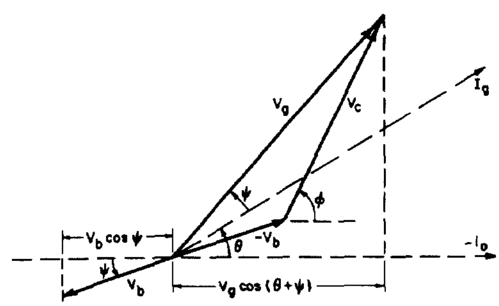

Fig. 3. Diagram showing vector addition of voltages in a beam-loaded cavity.